Essential Readings in Light Metals: Cast Shop for Aluminum Production.
Edited by John F. Grandfield and Dmitry G. Eskin.

NEW ELECTROMAGNETIC RHEOCASTERS FOR THE PRODUCTION OF THIXOTROPIC ALUMINUM ALLOY SLURRIES

Charles Vivès

Laboratoire de Magnétohydrodynamique
Université d'Avignon
F 84000, Avignon, France

Abstract

The working principle and the peculiarities of new electromagnetic rheocasters, which are based on the use of rotating permanent magnets and which allow the production of intense stirring in solidifying semi-solid alloy slurries, are described. These processes are likely to be applied to the direct continuous casting of billets, tubes and slabs and to the production of metal matrix composites. They are also characterized by a very low electric power consumption. Local measurement techniques are applied to the study of the evolution of the electromagnetic, hydrodynamic and thermal phenomena with the solid fraction, inside vigorously agitated melt-solid mixtures. Satisfactory performances concerning the microstructure of solidified aluminum thixotropic slurries (homogeneity, crystal shape, grain size, fraction of primary solid) were obtained.

Introduction

In the conventional rheocasting process, a solidifying alloy is generally mechanically stirred while in the freezing range. Thixotropic properties are possessed by this semi solid alloy, in which the solid phase has the structure of rounded particles suspended in a liquid matrix ; this binary mixture is likely to flow for high solid fractions, on the order of 0.6 |1-11|.

With respect to the conventional cast structures, the rheocast structures present manifold advantages : fine grained and uniformly distributed structure, reduced shrinkage, microporosity and cracking, improved mechanical properties. Moreover, the rheocasting technique is likely to be extended to emerging technologies, such as thixocasting and compocasting. In the thixocasting process, fine grain partially solidified metalworking alloys are intended to be formed, under pressure and after reheating, in the semi solid state. Metal matrix composites may be prepared by compocasting, the procedure consisting in the incorporation of third-phase particles of silicon carbide or alumina for instance, within a stirred semi-solid alloy slurry. This method promotes good bonding between the reinforcement and the matrix alloy and allows to achieve a very homogeneous particle distribution.

The mechanical stirring is commonly generated by means of augers, impellers, or multipaddle agitators mounted on a central rotating shaft |1-5|. However, the mechanical agitation approach is characterized by several specific and serious drawbacks. The slurry being here driven by viscous forces, the space occupied by the annulus formed between the rotor and the mixing chamber walls is necessarily confined and provides only a low volumetric rate of thixotropic slurry. Moreover, when the dimensions of the vessel containing the liquid-solid mixture are increased, dead zones marked by low shear rates becomes strongly viscous. It follows that, due to the coarsening of the crystals entrapped within these regions, the structure homogeneity is unsatisfactory. Furthermore, there are technological problems related to the erosion of the rotor, which is immersed into a very agressive medium, from the physico-chemical standpoint (such aluminum alloys, for instance) and can be responsible for an undesirable pollution of the metal. Lastly, it is generally not easy to associate mechanical agitation to a continuous casting system.

The aim of this work is to overcome these problems through the development of an electromagnetic device, allowing the production of an intense stirring in solidifying semi-solid alloy, whithout contact with the melt. This process, which is based on the use of rotating permanent magnets, is also characterized by a very low electric power consumption. Local measurement techniques are applied to the study of the evolution of the electromagnetic, hydrodynamic and thermal phenomena with the solid fraction, inside vigorously agitated melt-solid mixtures.

Working Principle

The schematic sketch presented in Figure 1 relates to a prototype where the magnets are arranged circumferentially around a cylindrical or an annular mold. This stirrer lends itself easily to static, semi-continuous and continuous casting of billets, tubes and slabs (Fig. 2).

Figure 1(a) shows the inductor, where the permanent magnets are alternately disposed according to a repetitive north-south azimuthal distribution. The rotor was driven, with an angular velocity wo, by an adjustable speed motor through a pulley-belt system permitting gradual variations of the speed of rotation N, ranging from 0 to 3000 r.p.m. When the inductor rotates, each point of the molten metal is subject to a variable magnetic field which generates induced electric currents. The main component of the current density is axial (J_Z) and the molten metal is set in rotation by azimuthal time-mean electromagnetic body forces, due to the interaction of the electric current J_Z and of the radial component of the magnetic field B_r.

The rotor consisted of four pairs of poles. Each pole, of 24 x 240 mm cross-section, was constituted by a row of ten parallelepipedic "ALNICO" permanent magnets of 30 mm in height and a 24 x 24 mm² square cross-sectional area. These magnets, magnetized along the greatest dimension, were embedded inside straight grooves machined along internal generatrices of a toroidal yoke made of stainless steel, with 130 and 165 mm inner and outer diameter, respectively.

The mold, made of stainless steel, was constituted by an interior cylinder of 70 and 73 mm inner and outer diameter and a coaxial external tube of 80 mm and 84 mm inner and outer diameter, respectively. An electric resistance, sunk in an insulating paste, was placed inside the annular gap formed between the two

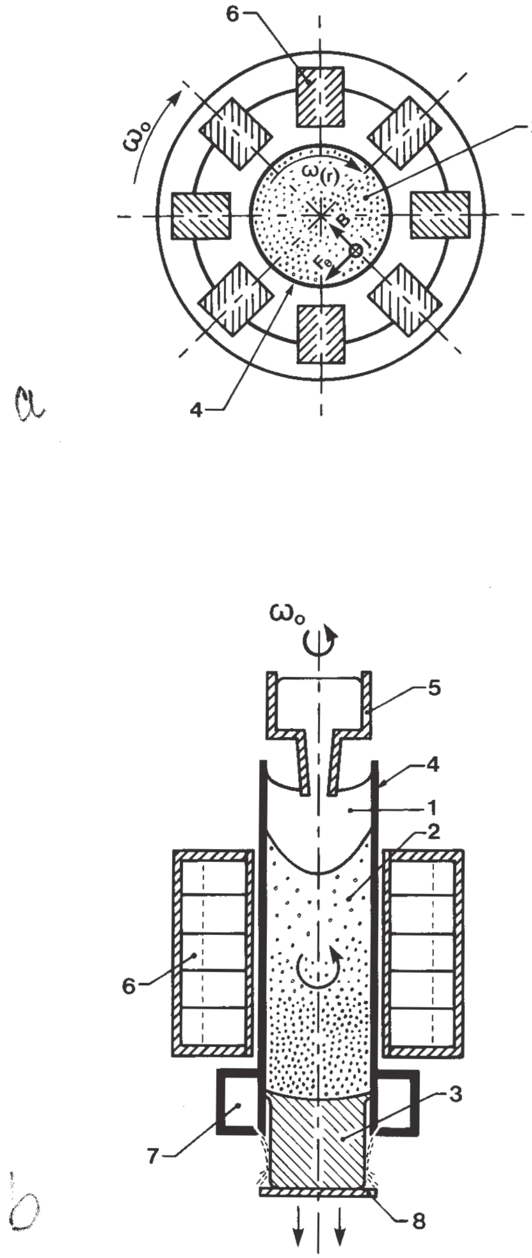

Figure 1 : Schematic sketch of an electromagnetic rheocaster equipped with an external rotor ; a) view from above, b) front view : 1) molten alloy, 2) slurry, 3) solidified alloy, 4) ingot mold, 5) spout, 6) magnets, 7) cooling water, 8) dummy bottom.

cylinders, in order to control the cooling rate and to prevent an untimely alloy freezing. During the rheocasting of aluminum alloy slurries, the temperature of the rotor was always lower than 200°C. Therefore, the magnetization of the "ALNICO" magnets was not appreciably affected by this augmentation of temperature. Moreover, periodical controls showed that the strength of the magnetic field generated by the inductor remained unchanged, even after several hundred hours of operation.

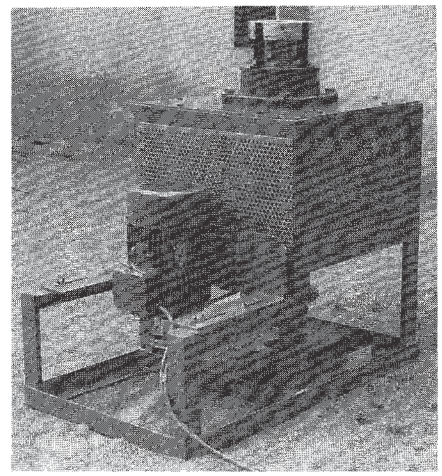

Figure 2 : Photograph of the MHD rhéocaster.

Various aluminum alloys were first melted using a direct-fired furnace and then poured into the mold. When a melt superheat on the order of 10°C was reached, the electromagnetic stirring was started and maintained until the end of the slurry motion. Rheocast aluminum alloys billets of 70 mm diameter and 240 mm height were produced according to this procedure. Samples were taken by means of a small spoon at various temperature during freezing, and either slowly solidified in air, or rapidly quenched by immersion in water.

The set of probes for magnetic field, current density and velocity measurements has been already described |12-14|. It should be pointed out that a thermocouple of 0.25 mm diameter was fastened to the electromagnetic velocity probe. This arrangement allowed to simultaneously follow, from recordings, the evolution with time of both the velocity and the temperature at a series of points within the solidifying slurry. Furthermore, experiments showed that when the solid fraction was not very high, the flow was highly turbulent. Accordingly, on account of the random character of the fluid motion, the velocity probe was connected to a microprocessor voltmeter able to take 200 readings per minute and also yield their average, highest and lowest values

Electromagnetic and Fluid Flow Phenomana

An example of profile of the tangential electromagnetic force, obtained from magnetic field, current density and phase shift measurements, is depicted in Figure 3. It is seen that the electromagnetic body forces are very strong, on the order of 7.5 10^5 $N.m^{-3}$ upon the mold wall and of 10^4 $N.m^{-3}$ at a distance of 2 cm from the wall. It results that this prototype is very efficient and the stirring of the alloy slurry is extremely vigorous in the melt, without dead zone. It has been verified that, at a given time, the temperature and, in turn, both the solid fraction and the apparent viscosity remain uniform throughout the binary mixture. Furthermore, no durable migration of primary solid particles towards the periphery of the billet, under the action of the centrifugal forces, was detected either from temperature measurements, or visually.

Owing to the medium confinement and to the high degrees of both the stirring intensity and temperature, methodical velocity measurements are particularly difficult here. Moreover, the working time of the sensors is limited to about 30 mn when they have been immersed into vigorously agitated molten aluminum

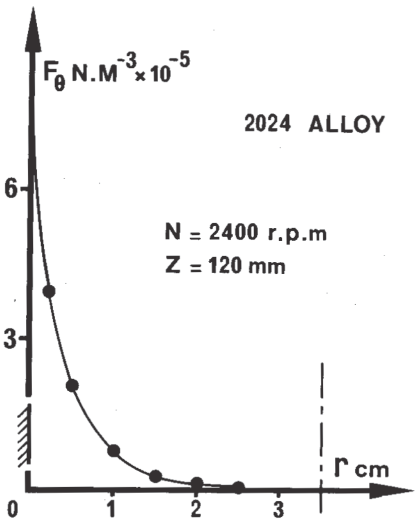

Figure 3 : Distribution of the tangential electromagnetic body force.

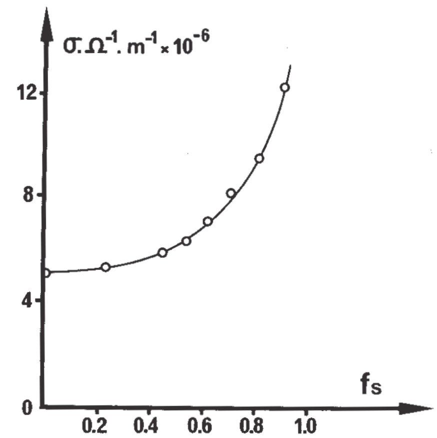

Figure 5 : Variation of the electrical conductivity of the 2024 aluminum alloy as a function of the solid fraction.

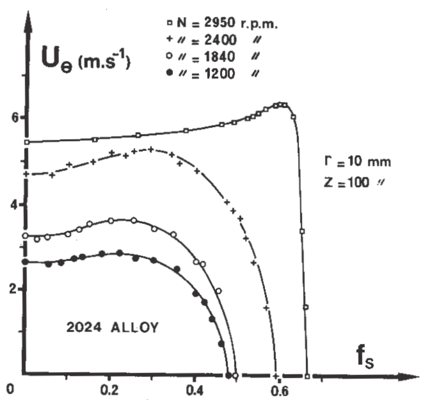

Figure 4 : Evolution of the tangential velocity component with the solid fraction, for various rotation speeds of the inductor.

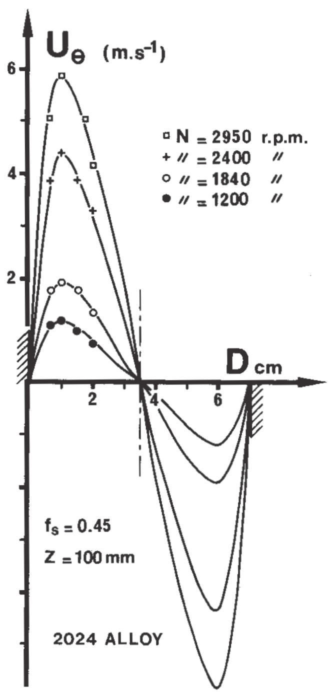

Figure 6 : Tangential velocity profiles plotted inside a 70 mm diameter 2024 aluminum alloy billet.

alloys, which are very agressive from the physicochemical standpoint.

Notwithstanding the fact that these local explorations are particularly difficult within aluminum alloy melts, experiments consisting in simultaneous recordings of velocity and temperature were carried out during the freezing of the solid-liquid mixture. Figure 4 shows the evolution of the tangential velocity U_θ, taken at a given point of a 2024 alloy slurry, with the solid fraction fs, for various rotation speeds of the inductor. It can be seen that the velocity increases up to a maximum, from which the semi solid alloy flow is rapidly slowed down. This maximum may be understood by the augmentation of the electrical conductivity σ of the binary mixture. The electrical conductivity-solid fraction relationship, related to the 2024 alloy, which was achieved in a previous experimental investigation |15|, is displayed in Figure 5. It is observed that when a solid fraction of 65 pct is reached, σ increases by 55 pct ; it follows that both the electric current density and the electromagnetic force increase nearly in the same proportion. Figure 6 presents velocity profiles plotted for a solid fraction of 0.45 and various rotation speeds N of the inductor. Obviously, the shear rate du/dr increases strongly with N ; for N = 2950 r.p.m., the shear rate is very steep in the vicinity of the mold wall (on the order of $10^{-3} s^{-1}$) and varies approximately linearly in the bulk of the melt. In addition, complementary tests have revealed the presence of a centripetal

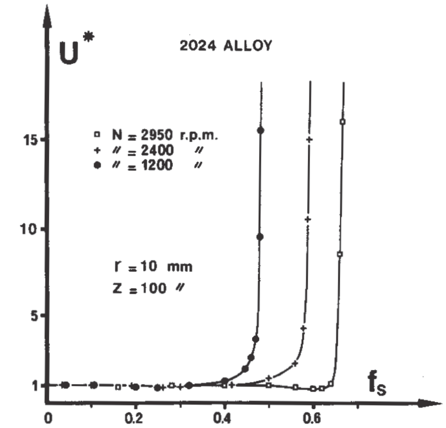

Figure 7 : Variation of the ratio U* of the molten alloy velocity to the velocity of the slurry, as a function of the solid fraction, for various inductor rotation speed.

velocity component which has a magnitude on the order of the azimuthal one.

Figure 7 shows the variation of the ratio U* of the molten alloy velocity (measured 10°C above the liquidus temperature) to the velocity of the slurry as a function of the solid fraction. The measurements were taken at a given point, for various stirring intensities. The variation of U* may be considered to be closely related to the evolution of a relative viscosity with the solid fraction. Curves of a similar trend, representing the variation of the relative viscosity as a function of the solid fraction for various shear stresses, were already previously obtained. In these experiments, the viscosity was determined from torque measurements using a Couette type viscometer, |1,2|. For the higher rotational speed N, it appears that the apparent viscosity of the melt-solid mixture remains practically unchanged up to a solid fraction of 0.65.

Metallographic Study

Two representative cases of solidification were mainly examined through the macro- and microstructure studies of a 2024 Alloy (liquidus: 638 °C, solidus 485 °C) and of a 1050 alloy (liquidus: 660 °C, solidus 635 °C) respectively characterized by a wide and a narrow freezing range.

Figure 8 presents comparisons between macrostructures corresponding to conventionally cast and rheocast ingots. Inspection of these slices, cut along horizontal cross-sections of 2024 and 1050 aluminum alloy billets of 70 mm diameter, reveals the appearance of a fine and homogeneous grain structure throughout the rheocast ingots.

Figure 9 shows the section of tubular ingots 240 mm high and of 43 and 70 mm, inner and outer diameter, respectively. The molten alloys were poured into an annular mold and then rheocast by means of the external inductor, rotating with a speed of 2400 r.p.m.

Examination of Figure 10, which displays 1050 alloy ingot tops (billets of 70 mm diameter), shows the dramatic reduction of the shrinkage effect by the electromagnetic rheocasting process. In spite that this alloy is close to the pure aluminum, it can be successfully rheocast. It should be mentioned that all the macro- and micro-structures presented here were obtained without inoculation of grain refiner master alloys and that this last finding may prove interesting for the electrical applications of the aluminum, which can be used to manufacture electric wires. In fact, the inoculation by a nucleating agent, which usually results in a decrease of the electric conductivity, can be totally avoided.

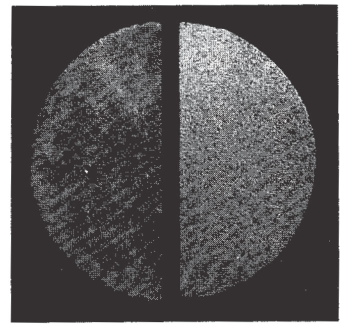

a)

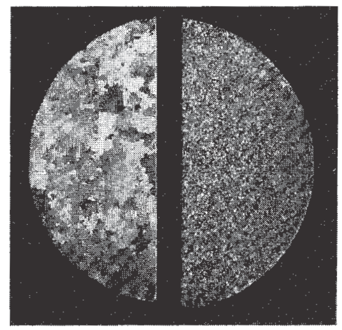

b)

Figure 8 : Macrostructures of aluminum alloy billets of 70 mm diameter, conventionally cast (left-hand side) and rheocast (right-hand side) ; a) 2024 alloy, b) 1050 alloy.

Figure 9 : Horizontal slices of tubular ingots of 70 mm outer diameter conventionally cast (left-hand side) and rheocast (right-hand side) : 2024 alloy (left) and 1050 alloy (right).

Figure 10 : Shrinkage effect on 1050 aluminum alloy billets of 70 mm diameter, conventionally cast (left-hand side) and rheocast (right-hand side).

It is well known that when an alloy is conventionally cast, without addition of grain refiners, its microstructure is generally characterized by a coarse columnar-dendritic crystallization. On the other hand, when the alloy is rheocast without water-quenching, the crystals forming the "primary solid" are approximately spheroidal in shape and uniformly distributed inside a solidifying liquid matrix. Moreover, a "secondary solid" consisting in a fine dendritic structure occurs in the matrix area, when the alloy is rheocast and rapidly water-quenched. These typical micro-structures, obtained with a 2024 aluminum alloy, can be found in Figure 11.

Figure 11(b), which relates to a sample water-quenched at a temperature corresponding to $f_S = 0.40$, exhibits a very fine structure, where the mean grain size of the primary solid is of 0.30 mm. In contrast, when the slurry is continuously sheared until the completion of the fluid consistency (i.e. when the alloy is getting stagnant) a marked grain coarsening, characterized by a mean grain size of 200 µm, occurs (Figure 11(c)). This new crystal structure, formed by sintering of particles, appears mainly when the stirring rate is slowed down |2|. It is obvious that the presence of such a "rosette structure" will be particularly favored in the final stages of solidification, when the shear rates are decidedly weakened (Fig. 4). When the globular structure is replaced by the rosette structure, the propensity of the particles to be driven with the remaining liquid phase flow is decidedly reduced, consequently, the decay of the flow rate of the binary mixture is increasingly accentuated. Inspection of Figure 4 reveals the dramatic acceleration of the evolution of this phenomenon when the solid fraction passes beyond 0.65.

Two other characteristic examples of rheocast microstructures, obtained with this MHD caster, and related to the 1050 and AS7G alloys are exhibited in Figure 12.

To achieve a homogeneous distribution of particles, or fibers, of small size in a metal matrix composite material, the mean grain size of the globular crystals constituting the primary solid must be very small. Hence, from the findings displayed in Figures 4 and 11, it is advised to cool the slurry rather rapidly when, (depending the rotation speed of the inductor) its solid fraction lies in the range 0.35-0.60. In the industrial rheocasting and compocasting operations, it is evident that the augmentation of the slurry stirring time results in a decreasing production rate. So, for the case of processes using M.H.D. casters, the heat extraction rate appears as a key parameter to control the microstructure of the rheocast materials.

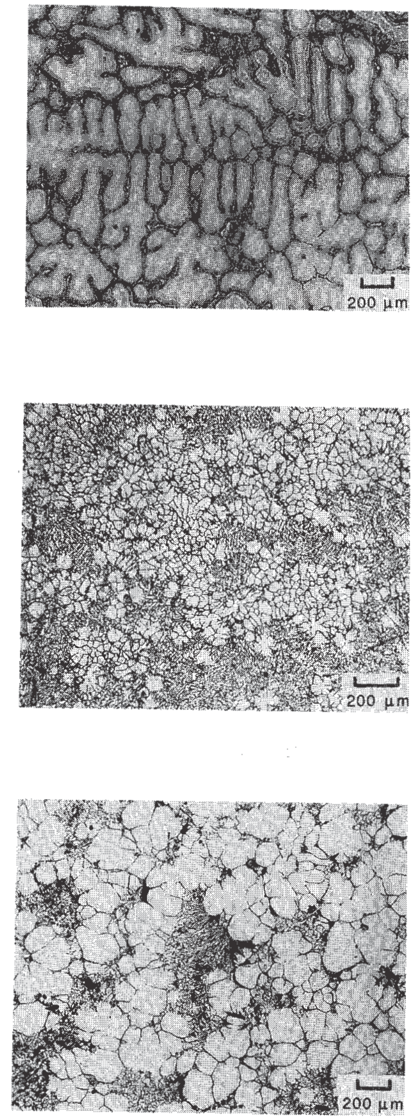

a)

b)

c)

Figure 11 : Microstructures of a 2024 aluminum alloy : a) as-cast material, b) rheocast material, 2400 r.p.m., fs = 0.40, water-quenched, c) rheocast material obtained at the completion of the slurry motion, 2400 r.p.m., fs = 0.55.

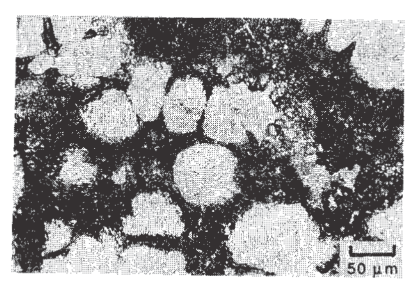

a)

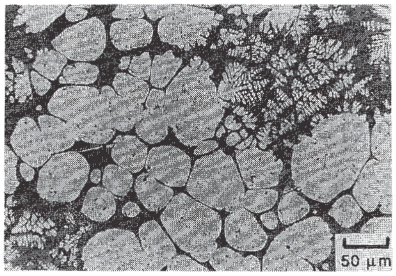

b)

Figure 12 : Microstructures of water-quenched rheocast samples : a) 1050 Al alloy, b) AS7G Al alloy.

Conclusions

Satisfactory performances concerning the microstructure of solidified aluminum alloy slurries (homogeneity, crystal shape, grain size and fraction of primary solid) were obtained using a new electromagnetic rheocaster based on the employment of rotating permanent magnets.

This technique presents manifold advantages :

(1) the direct continuous casting of billets, tubes and slabs is possible,

(2) The stirring is produced without any contact with the melt,

(3) compared to that of the multiphase motor stator the bulkiness of the inductor is weak, consequently important modifications of the standard D.C. casting equipment are not required ;

(4) The inductor height can be relatively important, on the order of 70 cm for instance, thus allowing an increasing stirring time during the slurry withdrawal. Moreover, the adjustment of the vertical temperature gradients within the binary mixture become easier ;

(5) The electric power consumption is insignificant (about 2 $kW.h^{-1}$ per ton), because the magnetic field is already generated by the permanent magnets, without any losses of active and reactive energies. It follows that the power factor is very close to one ;

(6) The cost of the electrical facilities is very low. Indeed, the equipment is merely reduced to an electric motor supplied with the main voltage.

Acknowledgements

The author wish to thank Serge Bercovici, Jean-Luc Meyer and Philippe Wallach of the Centre de Recherches de Voreppe, Pechiney, France, for their help.

References

1. D.B. Spencer, R. Mehrabian and M.C. Flemings, "Rheological Behavior of Sn - 15 pct Pb in the Crystallization Range", Met. Trans., 3 (1972), 1925-32.

2. P.A. Joly and R. Mehrabian, "The Rheology of a Partially Solidified Alloy", J. Met. Sci, 11 (1976), 1393-18.

3. M.C. Flemings, R. Mehrabian and R. G. Riek, U.S. Patent n° 3, 902, 544, issued September 1975.

4. J. Winter, J.A. Dantzig and D.E. Tyler, U.S. Patent n° 4, 434, 837, issued March 1984.

5. O.J. Ilegbusi and J. Szekely, "The Computation of the Velocity Field in Mechanically Agitated Melts for Turbulent and Non-Newtonian Regimes", Met. Trans., 21 B (1990), 183-90.

6. O.J. Ilegbusi and J. Szekely, "Mathematical Modeling of the Electromagnetic Stirring of Molten Metal-Solid Suspensions", Trans.ISIJ, 28 (1988), 97-103.

7. Ch. Vivès, French Patent n° 87 15817, issued November 1987.

8. Ch. Vivès, French Patent n° 88 04343, issued March 1988.

9. J.-J. A. Cheng, D. Apelian and R.D. Doherty, "Processing - Structure Characterisation of Rheocast IN-100 Super alloy", Met. Trans., 17 A (1986), 2049-62.

10. A. Tissier, D. Apelian, G. Regazzoni, "Magnesium Rheocasting : a Study of Processing - Microstructure Interactions", J. Mat. Sci., 25 (1990), 1184-96.

11. M.C. Flemings, "Behavior of Metal Alloys in the Semi-solid State", Met. Trans., 22 B (1991), 269-293.

12. R. Ricou and Ch. Vivès, "Local Velocity and Mass Transfer Measurements in Molten Metals using an Incorporated Magnet Probe", Int. J. Heat and Mass Transfer, 25 (10) (1982), 1579-88.

13. H.C. Lee, J.W. Evans and Ch. Vivès, "Velocity Measurements in Wood's Metal using an Incorporated Magnet Probe", Met. Trans. 15 B (1984), 734-36.

14. Ch. Vivès and R. Ricou, "Experimental Study of Continuous Electromagnetic Casting of Aluminum Alloys", Met. Trans., 16 B (1985), 377-84.

15. Ch. Vivès, "Hydrodynamic, Thermal and Crystallographical Effects of an Electromagnetically Driven Rotating Flow in Solidifying Aluminum Alloy Melts", Int. J. of Heat and Mass Transfer, 33 (12) (1990), 2585-98.